Highly efficient two-photon generation from a coherently pumped quantum dot embedded in a microcavity

J. K. Verma and P. K. Pathak
School of Basic Sciences, Indian Institute of Technology Mandi, Kamand, H.P. 175005, India
(Received 3 February 2016; revised manuscript received 4 August 2016; published 29 August 2016)

We propose two schemes to realize a highly efficient solid-state source of photon pairs using four-wave mixing and stimulated Raman adiabatic passage in a single quantum dot embedded in a microcavity. A resonant continuous-wave laser applied between biexciton and exciton states and a pulsed laser applied between a ground state and exciton state are utilized to facilitate coherent pumping. We show in the case of four-wave mixing that, although the probability of generating two photons in a cavity mode is small without cavity damping, two-photon-resonant emission is enhanced by cavity damping within the strong-coupling regime. For strong continuous-wave laser, a single photon from a pulsed laser and two-photon-resonant transition through a strongly coupled cavity mode lead to a (1+2)-type Raman transition through the generated Autler-Townes doublet. We also discuss the spectrum of the generated photon pair and the photon-photon correlations in the generated photon pair.

DOI: 10.1103/PhysRevB.94.085309

I. INTRODUCTION

Two-photon sources have a wide range of applications in atomic physics [1], quantum metrology [2], quantum information processing [3], quantum cryptography [4], in generating entangle photons [5], and heralded single-photon sources [6]. Until now, photon pairs employed in most of these experiments are generated by a parametric down conversion (PDC) [7] or by four-wave mixing in an optical fiber [8]. However, the number of generated photon pairs by such sources is random and the generation or collection efficiency is very low. Recently, there has been a lot of interest in generating a source of single-photon pairs [9–11] on demand, particularly for scalable quantum information processing and photonic technologies. Therefore sources using single emitters have become of great importance. The efficiency of these sources is greatly enhanced by strong coupling with a high-quality cavity; as a result, two-photon lasers [12,13] and masers [14] have been realized. For developing "on-chip" scalable solid-state photon sources, quantum dots (QDs) have emerged as a potential candidate. The QD can be strongly coupled in a photonic microcavity and can be grown precisely at the desired spatial location [15].

Two-photon emission is a weak nonlinear process and is only significant when single-photon processes are suppressed in the emitters. In a single emitter of upper energy level $|u\rangle$ and ground energy level $|g\rangle$, the resonant two-photon emission occurs at $\omega_{ug} = 2\omega$; where ω_{ug} is the transition frequency and ω is frequency of the emitted photons. The process proceeds through an intermediate state $|i\rangle$ which is far off-resonant to the single-photon transition. In QDs this situation occurs naturally because of large biexciton binding energy, when a single mode cavity having a frequency half of the biexciton-to-ground state transition frequency is coupled [10,11]. So far, the two-photon emission observed from a single QD coupled with a photonic crystal cavity relies on incoherent pumping [10]. The properties of the emitted photon pair strongly depend on the pumping mechanism and in an incoherently pumped source the efficiency and purity of emitted photons are degraded [16]. Such limitations of incoherent pumping have also been noticed by Ota *et al.* [10] in the demonstration of two-photon emission using a single QD coupled with a photonic crystal cavity. Because of inevitable excess scattering from the pump laser, coherent excitation of exciton levels in QD-cavity systems has been a challenging task and it becomes very hard to differentiate between scattered photons and the emitted photons. There have been some remarkable experiments demonstrating methods for coherent pumping of single QDs using an orthogonal excitation detection method in the photonic planar microcavity [17] and micropillar cavity [18]. In this paper, we propose a scheme for generating a source of single-photon pairs using coherent pumping which opens the possibility of four-wave mixing (FWM) and stimulated (1+2)-type Raman adiabatic passage (STIRAP) in a single QD embedded in a semiconductor photonic cavity [19–22]. Recently, FWM has been used for generating photon pairs using laser-cooled atomic ensembles [23]. Further, STIRAP has also been implemented using negatively charged QD for generating single photons with 99.5% indistinguishability [21] and there are theoretical proposals for generating entangled photon pairs [22]. In our scheme the pumping lasers and the emitted photon pair have not only a large difference in frequency but are also orthogonally polarized, which make them distinguishable.

Our paper is organized as follows. In Sec. II, we present our model for generating photon pairs and theoretical framework. Section III presents the population dynamics and spectrum of the generated photons. In Sec. IV we discuss photon-photon correlations. Finally, we conclude in Sec. V.

II. MODEL FOR GENERATING PHOTON PAIRS

We consider a single quantum dot embedded in a single mode photonic microcavity. The quantum dot has ground state $|g\rangle$ corresponding to no excitation, two optically active or "'bright" exciton energy levels $|x\rangle$ and $|y\rangle$ corresponding to total angular momentum $m = +1$ and -1, respectively, and a biexciton energy level $|u\rangle$ consisting of a pair of electrons with spins $\pm 1/2$ and a pair of holes with spins $\pm 3/2$. In Fig. 1, we

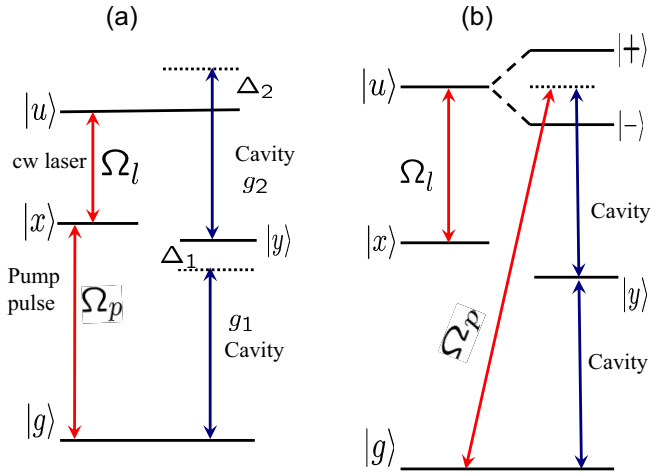

FIG. 1. (a) Schematic of the photon pair source using a single QD coupled with a y-polarized cavity mode, a cw laser (Ω_l), and a pump pulse laser [$\Omega_p(t)$] are used for coherent pumping, and (b) the equivalent scheme for STIRAP in the dressed state picture using a strong cw laser.

also consider the cavity mode, having polarization along the y direction, is coupled to $|u\rangle$ to $|y\rangle$ and $|y\rangle$ to $|g\rangle$ transitions with coupling constants g_1 and g_2, respectively. Because of the large biexciton binding energy in QDs, resonant coupling to both transitions $|u\rangle$ to $|y\rangle$ and $|y\rangle$ to $|g\rangle$ simultaneously with a single mode field is not possible. Therefore, we consider that the frequency of the cavity mode ω_c is chosen such that the two-photon resonant condition $\Delta_1 + \Delta_2 = 0$, $|\Delta_1| \gg g_1$, $|\Delta_2| \gg g_2$ is satisfied. Here, Δ_1 and Δ_2 are the detunings of the cavity mode to the $|u\rangle$ to $|y\rangle$ and $|y\rangle$ to $|g\rangle$ transitions, respectively. We use the notation $|\alpha,m\rangle$ for representing the combined state of quantum dot and cavity, where α represents the state of quantum dot and m represents the number of photons in the cavity mode. A two-photon transition between $|u,0\rangle$ and $|g,2\rangle$ via $|y,1\rangle$ takes place through the cavity mode and the single-photon transitions $|u,0\rangle \rightarrow |y,1\rangle$, $|y,1\rangle \rightarrow |g,2\rangle$, and $|y,0\rangle \rightarrow |g,1\rangle$ have negligible probabilities. The quantum dot can be pumped to biexciton state through less efficient two-photon absorption from a pump laser. Furthermore, we propose an innovative approach for a pumping mechanism, which makes two-photon emission in the cavity mode highly efficient, as follows. A resonant x-polarized cw laser is applied between the energy states $|u\rangle$ and $|x\rangle$ with coupling constant Ω_l and an x-polarized Gaussian pump pulse is applied between $|g\rangle$ and $|x\rangle$ with time-dependent coupling $\Omega_p(t)$. We note that a similar experiment using two x-polarized lasers for pumping a single QD coupled with a y-polarized cavity mode has been performed recently [24]. The Hamiltonian for the system is written as

$$\begin{aligned} h = {} & \hbar\omega_x|x\rangle\langle x| + \hbar\omega_y|y\rangle\langle y| + \hbar\omega_u|u\rangle\langle u| + \hbar\omega_c a^\dagger a \\ & + \hbar[(\Omega_l e^{-i\omega_l t}|u\rangle\langle x| + \Omega_p(t)e^{-i\omega_p t}|x\rangle\langle g| + g_1|y\rangle\langle g|a \\ & + g_2|u\rangle\langle y|a) + \text{H.c.}], \end{aligned} \tag{1}$$

where ω_α is the angular frequency corresponding to the QD energy level $|\alpha\rangle$, ω_l and ω_p are the frequencies of the cw laser and the pulsed laser, respectively, and H.c. refers to Hermitian conjugate. In the interaction picture, $H = e^{iH_0 t/\hbar} h e^{-iH_0 t/\hbar}$ where $H_0 = \hbar\omega_p|x\rangle\langle x| + \hbar(\omega_p + \omega_l)|u\rangle\langle u| + (\hbar/2)(\omega_p + \omega_l)|y\rangle\langle y| + (\hbar/2)(\omega_p + \omega_l)a^\dagger a$, the Hamiltonian (1) is rewritten as

$$\begin{aligned} H = {} & \hbar\Delta_p|x\rangle\langle x| + \frac{\hbar}{2}(\Delta_p + \Delta_l + \Delta_1 - \Delta_2)|y\rangle\langle y| \\ & + \hbar(\Delta_p + \Delta_l)|u\rangle\langle u| + \frac{\hbar}{2}(\Delta_p + \Delta_l - \Delta_1 - \Delta_2)a^\dagger a \\ & + \hbar[(\Omega_l|u\rangle\langle x| + \Omega_p(t)|x\rangle\langle g| + g_1|y\rangle\langle g|a + g_2|u\rangle\langle y|a) \\ & + \text{H.c.}], \end{aligned} \tag{2}$$

where Δ_p and Δ_l are the detunings of the pump pulse and the laser field. Initially, the QD is in the ground state $|g\rangle$ and the cavity mode has no photons. Depending on the strength of the cw laser, we find two different mechanisms for generating photon pairs through the cavity mode. First, when the applied resonant cw laser is weaker than the cavity induced resonant two-photon coupling, i.e., $\Omega_l \ll 2g_1g_2/\Delta_1$ [12], four-wave mixing occurs. A Gaussian pulse with properly selected amplitude Ω_p and detuning Δ_p generates a single-photon pair from the cavity mode with a probability larger than 0.9. In the second case, for a strong resonant cw-laser field ($\Omega_l \gg 2g_1g_2/\Delta_1$), applied between the $|x\rangle$ and $|u\rangle$, Autler-Townes doublets $|\pm\rangle = 1/\sqrt{2}(|u\rangle \pm |x\rangle)$ [25,26] are created. The energy separation between the states $|+\rangle$ and $|-\rangle$ is given by Ω_l. The states $|\pm\rangle$ are equally coupled to the ground state $|g\rangle$ through pump pulse. Further, they are also equally coupled to the state $|g,2\rangle$ through cavity induced two-photon resonant transitions via state $|y,1\rangle$. We note that equal coupling of Autler-Townes doublets $|\pm\rangle$ is necessary for efficient population transfer in STIRAP through multiple intermediate states $|\pm\rangle$ [27]. The two-photon transitions $|+\rangle \rightarrow |y,1\rangle \rightarrow |g,2\rangle$ and $|-\rangle \rightarrow |y,1\rangle \rightarrow |g,2\rangle$ interfere constructively and maximum population is transferred to $|g,2\rangle$ without populating $|y,1\rangle$. When a properly selected x-polarized Gaussian pump pulse is applied between QD states $|g\rangle$ and $|x\rangle$, the population is faithfully transferred to $|g,2\rangle$ through (1+2)-type Raman adiabatic passage [28], from where the photon pair is emitted from the leaky cavity mode.

For simulating the dynamics of the system, we perform master equation calculations in the density matrix representation:

$$\frac{\partial\rho}{\partial t} = -\frac{i}{\hbar}[H,\rho] - \frac{1}{2}\sum_\mu L_\mu^\dagger L_\mu \rho - 2L_\mu \rho L_\mu^\dagger + \rho L_\mu^\dagger L_\mu, \tag{3}$$

where L_μ are the Lindblad operators, with $L_1 = \sqrt{\gamma_1}|x\rangle\langle u|$, $L_2 = \sqrt{\gamma_1}|y\rangle\langle u|$, $L_3 = \sqrt{\gamma_2}|g\rangle\langle x|$, and $L_4 = \sqrt{\gamma_2}|g\rangle\langle y|$ corresponding to the spontaneous decays, and $L_5 = \sqrt{2\gamma_d}|u\rangle\langle u|$, $L_6 = \sqrt{\gamma_d}|x\rangle\langle x|$, and $L_7 = \sqrt{\gamma_d}|y\rangle\langle y|$ corresponding to the dephasing of biexciton and exciton states. The emission of photons from the cavity mode is given by the Lindblad operator $L_8 = \sqrt{\kappa}a$. We numerically integrate optical Bloch equations (A1)–(A10) for Gaussian pump pulse $\Omega_p(t)$ and calculate the probabilities of different states $\langle\alpha,m|\rho(t)|\alpha,m\rangle$ at any time t. We relegate the details of optical Bloch equations to the Appendix.

In our calculations we have used a fixed dephasing rate due to electron-phonon coupling. Although, in QD-cavity

systems electron-phonon interactions have a very complex nature, and different mechanisms such as pure dephasing [29], phonon-mediated transitions [30], and photon induced shake-up processes [31] have been proposed to understand observed features in different experimental conditions. However, for coherently excited QDs, coupling to continuum states in the wetting layer and shake-up processes due to charged excitons have been found negligible. Recent experiments at low temperatures, 5–10 K, using low power coherent excitation in resonant QD-cavity systems, have found that phenomenological exponential dephasing and exponential radiative decay are very well fitted with the data of Rabi oscillations and spectral linewidths. In a few remarkable experiments resonance fluorescence from doubly dressed QDs [32] and the resonant coupling of the Mollow sideband with cavity mode [33] have also been observed. For strongly driven off-resonant QD-cavity systems excitation induced dephasing has also been found to play a significant role in Mollow triplet sidebands broadening [34]. We predict that in our system excitation induced dephasing cannot play a significant role because we have proposed to use small values of Ω_l and Ω_p and two-photon resonant transitions through the cavity mode. Further, in the case of STIRAP, only those two-photon resonant transitions through the cavity mode which also satisfy the Raman resonance condition with pump pulse can occur [28]. We also remark that only the y-polarized resonant two-photon transition from exciton states are possible, and thus the presence of other background states, e.g, charged excitons, do not affect the evolution of the system. In fact, STIRAP has been successfully implemented between two selected motional states of trapped ions within a manifold of motional states [35].

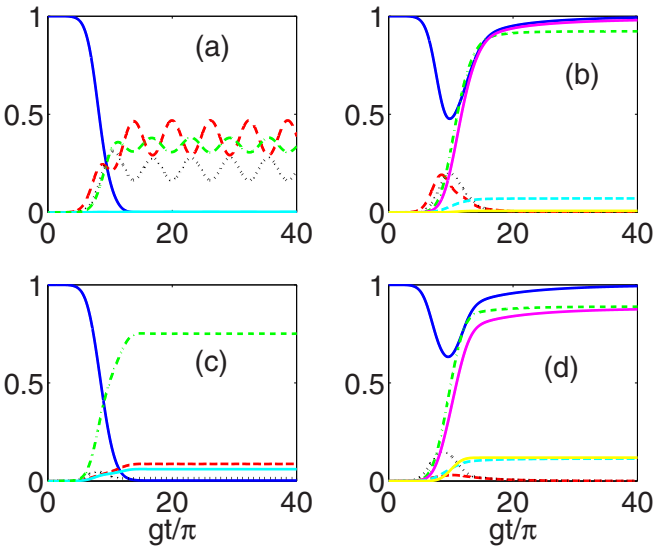

FIG. 2. The population in $\langle g,0|\rho|g,0\rangle$ (blue), $\langle x,0|\rho|x,0\rangle$ (red-dashed), and $\langle u,0|\rho|u,0\rangle$ (black-dotted). In (a) and (c), the population in $\langle y,1|\rho|y,1\rangle$ (cyan) and $\langle g,2|\rho|g,2\rangle + \langle x,2|\rho|x,2\rangle + \langle u,2|\rho|u,2\rangle$ (green dot-dashed). After introducing damping, $\gamma_1 = \gamma_2 = 10^{-3}g$, $\gamma_d = 10^{-2}g$, $\kappa = 0.5g$, in (b) and (d), the population in $\langle y,0|\rho|y,0\rangle$ (cyan) and the probabilities $P_1(t) = 2\kappa \int_0^t \langle g,2|\rho(t')|g,2\rangle + \langle x,2|\rho(t')|x,2\rangle + \langle u,2|\rho(t')|u,2\rangle dt'$ (green dot-dashed), $P_2(t) = \kappa \int_0^t \langle g,1|\rho(t')|g,1\rangle + \langle x,1|\rho(t')|x,1\rangle + \langle u,1|\rho(t')|u,1\rangle dt'$ (magenta), $P_3 = \kappa \int_0^t \langle y,1|\rho(t')|y,1\rangle dt'$ (cyan-dashed), and $P_4(t) = 3\kappa \int_0^t \langle g,3|\rho(t')|g,3\rangle dt'$ (yellow). The parameters are $g_1 = g_2 = g$, $\Delta_1 = -\Delta_2 = 4g$, $\Omega_p(t)/g = A_p \exp[-(t-2.5\tau)/\tau^2]$, $g\tau/\pi = 3.5$. For (a) and (b) $\Omega_l/g = 0.2$, $\Delta_p/g = 0.14$, $A_p = 0.132$. For (c) and (d) $\Omega_l/g = 1$, $\Delta_p/g = 0.46$, for (c) $A_p = 0.28$, and for (d) $A_p = 0.40$.

III. POPULATION DYNAMICS AND SPECTRUM OF THE EMITTED PHOTON PAIR

Next, we present our results of numerical simulations in Fig. 2. In simulations we include all possible states containing up to four photons in the cavity mode and neglect states having a higher number of photons. The y-polarized cavity mode satisfy two-photon resonance $\Delta_1 = -\Delta_2 = 4g_1 = 4g_2$, and the dot is driven by an x-polarized pump pulse and cw laser. We consider two different cases: first, when the driving cw laser is weaker than the cavity induced two-photon resonant coupling ($\Omega_l \ll 2g_1g_2/\Delta_1$), shown in Figs. 2(a) and 2(b); in this case the photon pair is generated through four-wave mixing. In the second case, when $\Omega_l \gg 2g_1g_2/\Delta_1$, shown in Figs. 2(c) and 2(d), the photon pair is generated through cavity-assisted STIRAP. In Figs. 2(a) and 2(c), results without spontaneous decay, cavity damping, and dephasing are plotted and in Figs. 2(b) and 2(d), results including cavity damping, spontaneous decay, and dephasing are plotted, using the same parameters, respectively. Considering all populated states of the system during evolution, we calculate probabilities of the emitting photon, $P_1 = 2\kappa \int_0^t \langle g,2|\rho(t')|g,2\rangle + \langle x,2|\rho(t')|x,2\rangle + \langle u,2|\rho(t')|u,2\rangle dt'$, $P_2 = \kappa \int_0^t \langle g,1|\rho(t')|g,1\rangle + \langle x,1|\rho(t')|x,1\rangle + \langle u,1|\rho(t')|u,1\rangle dt'$, $P_3 = \kappa \int_0^t \langle y,1|\rho(t')|y,1\rangle dt'$, and $P_4 = 3\kappa \int_0^t \langle g,3|\rho(t')|g,3\rangle dt'$ where P_1 is the probability of one photon emission from the generated photon pair, and P_2 is the sum of the probability of second photon emission from the generated photon pair and the probability of single-photon emission from $|y,0\rangle \rightarrow |g,1\rangle \rightarrow |g,0\rangle$. While P_3 is the probability of photon emission from state $|y,1\rangle$, and P_4 is the probability for photon emission from state $|g,3\rangle$, which is generated as a small population of $|g,1\rangle$ gets repumped in the system before it decays to $|g,0\rangle$. We found that $P_1(t) + P_3(t) \approx P_2(t) + P_4(t)$ when $t \rightarrow \infty$. In Figs. 2(a) and 2(c) we choose values of $\Omega_p(t)$ to achieve complete population transfer from initial state $|g,0\rangle$ and in Figs. 2(b) and 2(d) to achieve $P_1(t) + P_3(t) = 1$ in the long time limit. In Figs. 2(a) and 2(b) the required values of pump pulse $\Omega_p(t)$ are the same and in Fig. 2(c) the amplitude of pump pulse $\Omega_p(t)$ is slightly lower than the value in Fig. 2(d). We consider up to four photons in the cavity mode, i.e., up to state $|\alpha,4\rangle$ for $\alpha = g,x,u,y$. However, we found the probabilities of generating four-photon state $|g,4\rangle$ are < 0.05 and < 0.1 for the parameters used in Figs. 2(a) and 2(c), respectively. The populations of other states $|x,4\rangle$, $|u,4\rangle$, and $|y,4\rangle$ are negligible. It could be the effect of a photon blockade due to the Stark shifts produced by the presence of the photons in the cavity mode.

In Fig. 2(a), when there is no damping ($\gamma_1 = \gamma_2 = \gamma_d = \kappa = 0$), and a slowly varying x-polarized pump pulse $\Omega_p(t)$ is applied, the population from initial state $|g,0\rangle$ is completely transferred to states $|x,0\rangle$, $|u,0\rangle$, $|g,2\rangle$, $|x,2\rangle$,

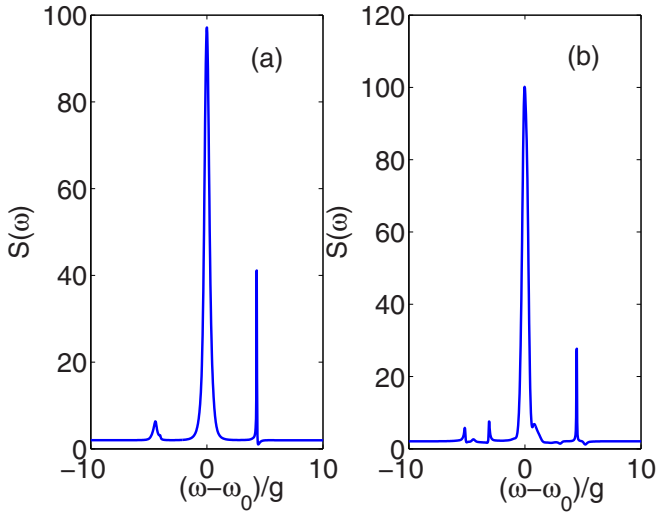

FIG. 3. Spectrum of the emitted photons through the cavity mode, (a) for parameters used in Fig. 2(b) and (b) for parameters used in Fig. 2(d).

and $|u,2\rangle$ without populating any other state significantly. The population in states $|x,2\rangle$ and $|u,2\rangle$ remains much less, ≈ 0.05. The probability of generating a photon pair inside cavity mode $\langle g,2|\rho(t)|g,2\rangle + \langle x,2|\rho(t)|x,2\rangle + \langle u,2|\rho(t)|u,2\rangle$ remains low (≈ 0.25). However, when the cavity damping such that $\kappa < g_1, g_2$ is introduced in Fig. 2(b) the population in $|x,0\rangle, |u,0\rangle$ goes to zero with a maximum around 0.2. We find that $P_2 \approx P_1 + P_3$ and $P_4 \approx 0$ in long time limit, which shows that the population in $|g,1\rangle$ is due to leakage of the photon from $|g,2\rangle$ as well as from the single-photon transition $|y,0\rangle \rightarrow |g,1\rangle$ and because the $\Omega_p \ll \kappa$ population from $|g,1\rangle$ could not get repumped into the system and decays to $|g,0\rangle$. We can estimate the efficiency of photon pair generation $\eta = \lim_{t\rightarrow\infty} \frac{P_1(t)-P_4(t)}{P_1(t)+P_3(t)} \approx \frac{P_1(t)-P_4(t)}{P_2(t)+P_4(t)}$. We find that in this case a single photon pair is generated by four-wave mixing with the efficiency higher than 0.9 per pump pulse. The probability of generating more than two photons per pulse is negligible.

In the second case of a stronger cw laser, we clearly notice the signature of cavity-assisted STIRAP which can be understood using the dressed state picture shown in Fig. 1(b). When a slowly varying pulse $\Omega_p(t)$ is applied between ground state and exciton state $|x\rangle$ most of the population is shifted to $|g,2\rangle$ [0.72 for the selected parameters used in Fig. 2(c)]. The populations in states $|x,0\rangle$, $|y,1\rangle$, and $|g,4\rangle$ remain less than 0.1 and less than 0.05 in all other states populated during evolution. In the presence of cavity damping, probabilities $P_1(t)$, $P_2(t)$, and $P_3(t)$ attain values 0.89, 0.88, and 0.11, respectively. However, the required amplitude of the pump pulse $\Omega_p(t)$ is comparable to cavity decay rate κ, therefore some population from $|g,1\rangle$ gets repumped into the system and we get $P_4(t) = 0.12$ in long time limit. The efficiency of photon pair emission is $\eta \approx 0.77$ for $\kappa = 0.5g$. In this case we also have a significant probability of generating three photon states per pulse.

In Fig. 3, we present the calculated cavity mode spectrum $S(\omega) = \int_0^\infty dt \int_0^\infty d\tau a^\dagger(t)a(t+\tau)\exp i\omega\tau$. The two-time correlation $a^\dagger(t)a(t+\tau)$ is calculated using a quantum regression theorem. We get one major peak corresponding to two-photon resonant emission at frequency $\omega_0 = (\omega_p + \omega_l)/2$ which is equal to the sum of the cavity mode frequency ω_c and a small contribution from Stark shifts. There are two tiny side peaks corresponding to single-photon emission from the cavity mode via cascaded decay of biexciton at $\omega - \omega_0 \approx \Delta_1, \Delta_2$. Further in strong driving limit, the peak corresponding to $\omega - \omega_0 \approx \Delta_2$ splits into two peaks separated by Ω_l, which is a signature of Autler-Townes doublets $|\pm\rangle$. In both cases the generated photon pair can be filtered using frequency filters centered around the frequency of the cavity mode.

IV. PHOTON-PHOTON CORRELATIONS

We present the results of photon-photon correlations in Fig. 4. We calculate two-photon correlation $G^2(\tau) = \int_0^\infty dt a^\dagger(t)a^\dagger(t+\tau)a(t+\tau)a(t)$ and three-photon correlation $G^3(\tau,\tau') = \int_0^\infty dt a^\dagger(t)a^\dagger(t+\tau)a^\dagger(t+\tau+\tau')a(t+\tau+\tau')a(t+\tau)a(t)$ using the quantum regression theorem and Eq. (3). In our system two types of processes are involved for photon emission: resonant two-photon emission which leads to a photon pair emission around cavity frequency and cavity modified spontaneous biexciton-exciton cascade decay leading to slow emission of two photons of frequencies $(\omega - \omega_0) \approx \Delta_1, \Delta_2$. In Figs. 4(a) and 4(b), we find the first peak around $\tau \approx 0$, corresponding to simultaneous resonant emission of two photons, followed by extended tail, corresponding to slow emission of two photons in cascaded decay. In Figs. 4(c) and 4(d), a three-photon correlation function is plotted corresponding to the parameters used in Figs. 4(a) and 4(b). Two main conclusions can be drawn from (c): first there is negligible probability of generating more than two photons in the cavity mode as G^3 has zero value for $\tau = \tau' \approx 0$. Also, there is no temporal overlapping between resonant photon pair generation and photons generated in cascaded decay; two-photon resonant emission finishes first

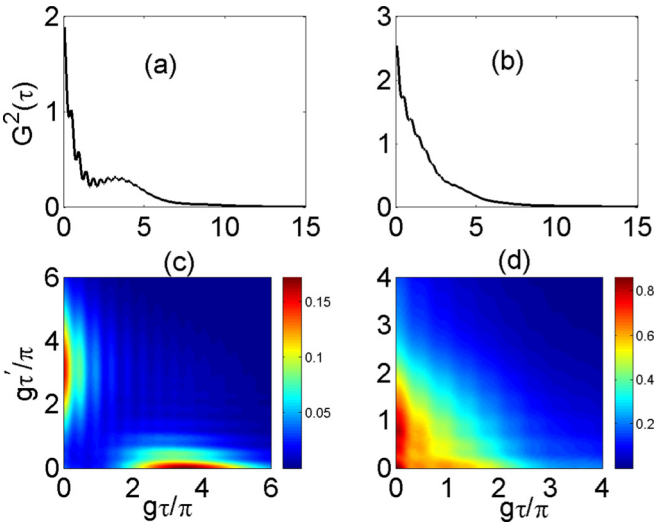

FIG. 4. Two-photon correlation function $G^2(\tau)$ is plotted in (a) and (b), and three-photon correlation function $G^3(\tau,\tau')$ is shown in (c) and (d). The parameters for (a) and (c) are the same as in Fig. 2(b) and the parameters for (b) and (d) are the same as in Fig. 2(d).

[see Fig. 2(b)]. Second, the nonzero values of G^3 lie along the axis, confirming that two photons in resonant process are emitted simultaneously and two photons in cascaded decay are emitted slowly. In Fig. 4(d), we see that G^3 is nonzero for $\tau = \tau' \approx 0$ which shows a finite probability of generating a $|g,3\rangle$ state in the STIRAP process. Other features are the same as in Fig. 4(c).

V. CONCLUSIONS

We have presented a method for efficient resonant excitation in a single neutral QD embedded in a photonic microcavity which enables four-wave mixing and (1+2)-type STIRAP depending on the intensity of pumping cw laser. The efficiency of generating photon pairs could be very large in both cases, thus opening up the possibility of realizing a solid-state "on demand" source of photon pair. We found that using low values of cw laser and pump pulse $[\Omega_l, \Omega_p(t) \ll \kappa]$, in four-wave mixing the efficiency of generating single-photon pairs could be larger than 0.9 per pulse and there is negligible probability of generating more than two photons in the cavity mode. In the case of STIRAP, the required amplitude of pump pulse becomes comparable to cavity damping, therefore there is a finite probability of generating three photons in the cavity mode.

ACKNOWLEDGMENTS

We acknowledge financial support from SERB, Department of Science and Technology (DST), India [Project Grant No. SR/FTP/PS-122/2011].

APPENDIX: OPTICAL BLOCH EQUATIONS

Using density operator (3) and notation $\partial\langle\alpha,n|\rho|\beta,m\rangle/\partial t = \dot{\rho}_{\alpha\beta}(n,m)$, where α,β represent the energy levels in a QD and m,n represent the number of photons in the cavity mode, the optical Bloch equations are given by

$$\begin{aligned}\dot{\rho}_{gg}(n,m) = &-\frac{i}{2}(n-m)(\Delta_p+\Delta_l-\Delta_1-\Delta_2)\rho_{gg}(n,m) - i\Omega_p^*\rho_{xg}(n,m) + i\Omega_p\rho_{gx}(n,m) - ig_1\sqrt{n}\rho_{yg}(n-1,m)\\ &+ ig_1\sqrt{m}\rho_{gy}(n,m-1) + \gamma_2\rho_{yy}(n,m) + \gamma_2\rho_{xx}(n,m) - \frac{\kappa}{2}(n+m)\rho_{gg}(n,m)\\ &+ \kappa\sqrt{(n+1)(m+1)}\rho_{gg}(n+1,m+1),\end{aligned} \tag{A1}$$

$$\begin{aligned}\dot{\rho}_{xx}(n,m) = &-\frac{i}{2}(n-m)(\Delta_p+\Delta_l-\Delta_1-\Delta_2)\rho_{xx}(n,m) - i\Omega_l^*\rho_{ux}(n,m) + i\Omega_l\rho_{xu}(n,m) - i\Omega_p\rho_{gx}(n,m)\\ &+ i\Omega_p^*\rho_{xg}(n,m) - \gamma_2\rho_{xx}(n,m) + \gamma_1\rho_{uu}(n,m) - \frac{\kappa}{2}(n+m)\rho_{xx}(n,m) + \kappa\sqrt{(n+1)(m+1)}\rho_{xx}(n+1,m+1),\end{aligned} \tag{A2}$$

$$\begin{aligned}\dot{\rho}_{uu}(n,m) = &-\frac{i}{2}(n-m)(\Delta_p+\Delta_l-\Delta_1-\Delta_2)\rho_{uu}(n,m) + i\Omega_l^*\rho_{ux}(n,m) - ig_2\sqrt{n+1}\rho_{yu}(n+1,m) - i\Omega_l\rho_{xu}(n,m)\\ &+ ig_2\sqrt{m+1}\rho_{uy}(n,m+1) - 2\gamma_1\rho_{uu}(n,m) - \frac{\kappa}{2}(n+m)\rho_{uu}(n,m) + \kappa\sqrt{(n+1)(m+1)}\rho_{uu}(n+1,m+1)\end{aligned} \tag{A3}$$

$$\begin{aligned}\dot{\rho}_{yy}(n,m) = &-\frac{i}{2}(n-m)(\Delta_p+\Delta_l-\Delta_1-\Delta_2)\rho_{yy}(n,m) - ig_2\sqrt{n}\rho_{uy}(n-1,m) + ig_2\sqrt{m}\rho_{yu}(n,m-1)\\ &- ig_1\sqrt{n+1}\rho_{gy}(n+1,m) + ig_1\sqrt{m+1}\rho_{yg}(n,m+1) - \frac{\kappa}{2}(n+m)\rho_{yy}(n,m) - \gamma_2\rho_{yy}(n,m) + \gamma_1\rho_{uu}(n,m)\\ &+ \kappa\sqrt{(n+1)(m+1)}\rho_{yy}(n+1,m+1),\end{aligned} \tag{A4}$$

$$\begin{aligned}\dot{\rho}_{yg}(n,m) = &-\frac{i}{2}(n-m)(\Delta_p+\Delta_l-\Delta_1-\Delta_2)\rho_{yg}(n,m) - \frac{i}{2}(\Delta_p+\Delta_l+\Delta_1-\Delta_2)\rho_{yg}(n,m) - ig_2\sqrt{n}\rho_{ug}(n-1,m)\\ &- ig_1\sqrt{n+1}\rho_{gg}(n+1,m) + g_1\sqrt{m}\rho_{yy}(n,m-1) + i\Omega_p\rho_{yx}(n,m) - \frac{\kappa}{2}(n+m)\rho_{yg}(n,m) - \frac{(\gamma_2+\gamma_d)}{2}\rho_{yg}(n,m)\\ &+ \kappa\sqrt{(n+1)(m+1)}\rho_{yg}(n+1,m+1),\end{aligned} \tag{A5}$$

$$\begin{aligned}\dot{\rho}_{xg}(n,m) = &-\frac{i}{2}(n-m)(\Delta_p+\Delta_l-\Delta_1-\Delta_2)\rho_{xg}(n,m) - i\Delta_p\rho_{xg}(n,m) - i\Omega_p[\rho_{gg}(n,m)-\rho_{xx}(n,m)] - i\Omega_l^*\rho_{ug}(n,m)\\ &+ ig_1\sqrt{m}\rho_{xy}(n,m-1) - \frac{(\gamma_2+\gamma_d)}{2}\rho_{xg}(n,m) - \frac{\kappa}{2}(n+m)\rho_{xg}(n,m) + \kappa\sqrt{(n+1)(m+1)}\rho_{xg}(n+1,m+1),\end{aligned} \tag{A6}$$

$$\dot{\rho}_{ug}(n,m) = -\frac{i}{2}(n-m)(\Delta_p+\Delta_l-\Delta_1-\Delta_2)\rho_{ug}(n,m) - i(\Delta_p+\Delta_l)\rho_{ug}(n,m) - i\Omega_l\rho_{xg}(n,m) + i\Omega_p\rho_{ux}(n,m)$$
$$- ig_2\sqrt{n+1}\rho_{yg}(n+1,m) + ig_1\sqrt{m}\rho_{uy}(n,m-1) - \frac{\kappa}{2}(n+m)\rho_{ug}(n,m) - (\gamma_1+\gamma_d)\rho_{ug}(n,m)$$
$$+\kappa\sqrt{(n+1)(m+1)}\rho_{ug}(n+1,m+1), \tag{A7}$$

$$\dot{\rho}_{ux}(n,m) = -\frac{i}{2}(n-m)(\Delta_p+\Delta_l-\Delta_1-\Delta_2)\rho_{ux}(n,m) - i\Delta_l\rho_{ux}(n,m) - i\Omega_l[\rho_{xx}(n,m)-\rho_{uu}(n,m)] + i\Omega_p^*\rho_{ug}(n,m)$$
$$- ig_2\sqrt{n+1}\rho_{yx}(n+1,m) - \frac{(2\gamma_1+\gamma_2+3\gamma_d)}{2}\rho_{ux}(n,m) - \frac{\kappa}{2}(n+m)\rho_{ux}(n,m)$$
$$+\kappa\sqrt{(n+1)(m+1)}\rho_{ux}(n+1,m+1), \tag{A8}$$

$$\dot{\rho}_{uy}(n,m) = -\frac{i}{2}(n-m)(\Delta_p+\Delta_l-\Delta_1-\Delta_2)\rho_{uy}(n,m) - \frac{i}{2}(\Delta_p+\Delta_l-\Delta_1+\Delta_2)\rho_{uy}(n,m) - i\Omega_l\rho_{xy}(n,m)$$
$$- ig_2\sqrt{n+1}\rho_{yy}(n+1,m) + ig_2\sqrt{m}\rho_{uu}(n,m-1) + ig_1\sqrt{m+1}\rho_{ug}(n,m+1) - \frac{(2\gamma_1+\gamma_2+3\gamma_d)}{2}\rho_{uy}(n,m)$$
$$-\frac{\kappa}{2}(n+m)\rho_{uy}(n,m) + \kappa\sqrt{(n+1)(m+1)}\rho_{uy}(n+1,m+1), \tag{A9}$$

$$\dot{\rho}_{yx}(n,m) = -\frac{i}{2}(n-m)(\Delta_p+\Delta_l-\Delta_1-\Delta_2)\rho_{yx}(n,m) - \frac{i}{2}(\Delta_l-\Delta_p+\Delta_1-\Delta_2)\rho_{yx}(n,m)$$
$$- ig_2\sqrt{n}\rho_{ux}(n-1,m) - ig_1\sqrt{n+1}\rho_{gx}(n+1,m) + i\Omega_l\rho_{yu}(n,m) + i\Omega_p^*\rho_{yg}(n,m) - (\gamma_2+\gamma_d)\rho_{yx}(n,m)$$
$$-\frac{\kappa}{2}(n+m)\rho_{yx}(n,m) + \kappa\sqrt{(n+1)(m+1)}\rho_{yx}(n+1,m+1), \tag{A10}$$

[1] Christian G. Parthey, A. Matveev, J. Alnis, B. Bernhardt, A. Beyer, R. Holzwarth, A. Maistrou, R. Pohl, K. Predehl, T. Udem, T. Wilken, N. Kolachevsky, M. Abgrall, D. Rovera, C. Salomon, P. Laurent, and T. W. Hänsch, Phys. Rev. Lett. **107**, 203001 (2011); M. Niering, R. Holzwarth, J. Reichert, P. Pokasov, T. Udem, M. Weitz, T. W. Hänsch, P. Lemonde, G. Santarelli, M. Abgrall, P. Laurent, C. Salomon, and A. Clairon, *ibid.* **84**, 5496 (2000).

[2] B. Bell, S. Kannan, A. McMillan, A. S. Clark, W. J. Wadsworth, and J. G. Rarity, Phys. Rev. Lett. **111**, 093603 (2013); J. G. Rarity, P. R. Tapster, E. Jakeman, T. Larchuk, R. A. Campos, M. C. Teich, and B. E. A. Saleh, *ibid.* **65**, 1348 (1990); V. Giovannetti, S. Lloyd, and L. Maccone, Nat. Photonics **5**, 222 (2011).

[3] E. V. Moreva, G. A. Maslennikov, S. S. Straupe, and S. P. Kulik, Phys. Rev. Lett. **97**, 023602 (2006); A. Rossi, G. Vallone, A. Chiuri, F. De Martini, and P. Mataloni, *ibid.* **102**, 153902 (2009); E. Nagali, D. Giovannini, L. Marrucci, S. Slussarenko, E. Santamato, and F. Sciarrino, *ibid.* **105**, 073602 (2010); B. P. Lanyon, T. J. Weinhold, N. K. Langford, J. L. O'Brien, K. J. Resch, A. Gilchrist, and A. G. White, *ibid.* **100**, 060504 (2008).

[4] Y. I. Bogdanov, M. V. Chekhova, S. P. Kulik, G. A. Maslennikov, A. A. Zhukov, C. H. Oh, and M. K. Tey, Phys. Rev. Lett. **93**, 230503 (2004).

[5] R. M. Stevenson, R. J. Young, P. Atkinson, K. Cooper, D. A. Ritchie, and A. J. Shields, Nature (London) **439**, 179 (2006); P. K. Pathak and S. Hughes, Phys. Rev. B **79**, 205416 (2009); **80**, 155325 (2009).

[6] M. Davanço, J. R. Ong, A. B. Shehata, A. Tosi, I. Agha, S. Assefa, F. Xia, W. M. J. Green, S. Mookherjea, and K. Srinivasan, Appl. Phys. Lett. **100**, 261104 (2012).

[7] J. Fekete, D. Rieländer, M. Cristiani, and H. de Riedmatten, Phys. Rev. Lett. **110**, 220502 (2013).

[8] M. Fiorentino, P. L. Voss, J. E. Sharping, and P. Kumar, IEEE Photon. Technol. Lett. **14**, 983 (2002).

[9] W. C. Jiang, X. Lu, J. Zhang, O. Painter, and Q. Lin, Opt. Express **23**, 20884 (2015).

[10] Y. Ota, S. Iwamoto, N. Kumagai, and Y. Arakawa, Phys. Rev. Lett. **107**, 233602 (2011).

[11] E. del Valle, A. Gonzalez-Tudela, E. Cancellieri, and F. P. Laussy, New J. Phys. **13**, 113014 (2011).

[12] E. del Valle, S. Zippilli, F. P. Laussy, A. Gonzalez-Tudela, G. Morigi, and C. Tejedor, Phys. Rev. B **81**, 035302 (2010).

[13] Daniel J. Gauthier, Qilin Wu, S. E. Morin, and T. W. Mossberg, Phys. Rev. Lett. **68**, 464 (1992); C. Z. Ning, *ibid.* **93**, 187403 (2004).

[14] M. Brune, J. M. Raimond, P. Goy, L. Davidovich, and S. Haroche, Phys. Rev. Lett. **59**, 1899 (1987); M. Brune, J. M. Raimond, and S. Haroche, Phys. Rev. A **35**, 154 (1987); L. Davidovich, J. M. Raimond, M. Brune, and S. Haroche, *ibid.* **36**, 3771 (1987).

[15] J. P. Reithmaier, G. Sek, A. Löffler, C. Hofmann, S. Kuhn, S. Reitzenstein, L. V. Keldysh, V. D. Kulakovskii, T. L. Reinecke, and A. Forchel, Nature (London) **432**, 197 (2004); T. Yoshie, A. Scherer, J. Hendrickson, G. Khitrova, H. M. Gibbs, G. Rupper, C. Ell, O. B. Shchekin, and D. G. Deppe, *ibid.* **432**, 200 (2004).

[16] A. Kiraz, M. Atatüre, and A. Imamoglu, Phys. Rev. A **69**, 032305 (2004); J. P. Torres, K. Banaszek, and I. A. Walmsley, Prog. Opt. **56**, 227 (2011).

[17] E. B. Flagg, A. Muller, J. W. Robertson, S. Founta, D. G. Deppe, M. Xiao, W. Ma, G. J. Salamo, and C. K. Shih, Nat. Phys. **5**, 203 (2009); E. B. Flagg, A. Muller, S. V. Polyakov, A. Ling, A. Migdall, and G. S. Solomon, Phys. Rev. Lett. **104**, 137401 (2010).

[18] S. Ates, S. M. Ulrich, S. Reitzenstein, A. Löffler, A. Forchel, and P. Michler, Phys. Rev. Lett. **103**, 167402 (2009); S. Ates, S. M. Ulrich, A. Ulhaq, S. Reitzenstein, A. Löffler, S. Höfling, A. Forchel, and P. Michler, Nat. Photonics **3**, 724 (2009).

[19] P. K. Pathak and S. Hughes, Phys. Rev. B **82**, 045308 (2010).

[20] Yu He, Yu-Ming He, Y.-J. Wei, X. Jiang, M.-C. Chen, F.-L. Xiong, Y. Zhao, Christian Schneider, Martin Kamp, Sven Höfling, Chao-Yang Lu, and Jian-Wei Pan, Phys. Rev. Lett. **111**, 237403 (2013); G. Fernandez, T. Volz, R. Desbuquois, A. Badolato, and A. Imamoglu, *ibid.* **103**, 087406 (2009).

[21] Y.-J. Wei, Y.-M. He, M.-C. Chen, Y.-N. Hu, Y. He, D. Wu, C. Schneider, M. Kamp, S. Hofling, C.-Y. Lu, and J.-W. Pan, Nano Lett. **14**, 6515 (2014).

[22] R. García-Maraver, K. Eckert, R. Corbalán, and J. Mompart, Phys. Rev. A **74**, 031801(R) (2006); J. Phys. B **41**, 045505 (2008).

[23] B. Srivathsan, G. K. Gulati, B. Chng, G. Maslennikov, D. Matsukevich, and C. Kurtsiefer, Phys. Rev. Lett. **111**, 123602 (2013); J. K. Thompson, J. Simon, H. Loh, and V. Vuletic, Science **313**, 74 (2006).

[24] F. Hargart, M. Muller, K. Roy-Choudhury, S. L. Portalupi, C. Schneider, S. Hofling, M. Kamp, S. Hughes, and P. Michler, Phys. Rev. B **93**, 115308 (2016).

[25] S. J. Boyle, A. J. Ramsay, A. M. Fox, M. S. Skolnick, A. P. Heberle, and M. Hopkinson, Phys. Rev. Lett. **102**, 207401 (2009).

[26] A. Muller, W. Fang, John Lawall, and G. S. Solomon, Phys. Rev. Lett. **101**, 027401 (2008).

[27] N. V. Vitanov and S. Stenholm, Phys. Rev. A **60**, 3820 (1999).

[28] L. P. Yatsenko, S. Guérin, T. Halfmann, K. Böhmer, B. W. Shore, and K. Bergmann, Phys. Rev. A **58**, 4683 (1998); S. Guérin, L. P. Yatsenko, T. Halfmann, B. W. Shore, and K. Bergmann, *ibid.* **58**, 4691 (1998).

[29] B. Krummheuer, V. M. Axt, and T. Kuhn, Phys. Rev. B **65**, 195313 (2002); J. Förstner, C. Weber, J. Danckwerts, and A. Knorr, Phys. Rev. Lett. **91**, 127401 (2003).

[30] P. Borri, W. Langbein, S. Schneider, U. Woggon, R. L. Sellin, D. Ouyang, and D. Bimberg, Phys. Rev. Lett. **87**, 157401 (2001).

[31] M. Kaniber, A. Laucht, A. Neumann, J. M. Villas-Bôas, M. Bichler, M.-C. Amann, and J. J. Finley, Phys. Rev. B **77**, 161303(R) (2008); M. Winger, T. Volz, G. Tarel, S. Portolan, A. Badolato, K. J. Hennessy, E. L. Hu, A. Beveratos, J. Finley, V. Savona, and A. Imamoglu, Phys. Rev. Lett. **103**, 207403 (2009).

[32] Y. He, Y.-M. He, J. Liu, Y.-J. Wei, H. Y. Ramírez, M. Atatüre, C. Schneider, M. Kamp, S. Höfling, C.-Y. Lu, and J.-W. Pan, Phys. Rev. Lett. **114**, 097402 (2015).

[33] H. Kim, T. C. Shen, K. Roy-Choudhury, G. S. Solomon, and W. Waks, Phys. Rev. Lett. **113**, 027403 (2014).

[34] S. M. Ulrich, S. Ates, S. Reitzenstein, A. Loffler, A. Forchel, and P. Michler, Phys. Rev. Lett. **106**, 247402 (2011); C. Roy and S. Hughes, *ibid.* **106**, 247403 (2011); A. Majumdar, E. D. Kim, Y. Gong, M. Bajcsy, and J. Vuckovic, Phys. Rev. B **84**, 085309 (2011); L. Monniello, C. Tonin, R. Hostein, A. Lemaitre, A. Martinez, V. Voliotis, and R. Grousson, Phys. Rev. Lett. **111**, 026403 (2013).

[35] J. I. Cirac, R. Blatt, and P. Zoller, Phys. Rev. A **49**, R3174 (1994); D. M. Meekhof, C. Monroe, B. E. King, W. M. Itano, and D. J. Wineland, Phys. Rev. Lett. **76**, 1796 (1996).